Tunable self-shifting Bloch modes in anisotropic hexagonal photonic lattices

Sheng Liu,[1] Yi Hu,[2] Peng Zhang,[3,4] Xuetao Gan,[1] Cibo Lou,[2] Daohong Song,[2] Jianlin Zhao,[1,*] Jingjun Xu,[2] and Zhigang Chen[2,3]

[1]*Key Laboratory of Space Applied Physics and Chemistry, Ministry of Education; and Shaanxi Key Laboratory of Optical Information Technology, School of Science, Northwestern Polytechnical University, 710072 Shaanxi, China*

[2]*Key Laboratory of Weak-Light Nonlinear Photonics, Ministry of Education; and TEDA Applied Physics School, Nankai University, 300457 Tianjin, China*

[3]*Department of Physics and Astronomy, San Francisco State University, San Francisco, California 94132, USA*

[4]*Current address: NSF Nanoscale Science and Engineering Center, University of California, Berkeley, California 94720, USA*

*Corresponding author: jlzhao@nwpu.edu.cn

We study controllable self-shifting Bloch modes in anisotropic hexagonal photonic lattices. The shifting results from a deformed band structure due to deformation of the index distribution in each unit cell. By reconfiguration of the index profile of the unit cell, the direction in which the Bloch modes move can be controlled. Our theoretical predictions are experimentally demonstrated in hexagonal lattices optically induced in an anisotropic nonlinear crystal.   © 2012 Optical Society of America

OCIS codes: 050.1940, 080.1238.

Wave propagation in optical periodic structures has received considerable attention in the past decade. In a typical photonic lattice, the ability to manipulate light relies on the photonic bandgap design [1,2]. Many interesting phenomena have been observed, such as anomalous diffraction and refraction [3], conical diffraction [4,5], and symmetry-breaking diffraction [6]. According to the Floquet—Bloch theorem, beam propagation in photonic lattices can be analyzed from spatially extended Bloch waves as a complete orthogonal set of allowed eigenmodes of the lattice [2]. In uniform photonic lattices, localized modes characterized by Bloch waves are crucial for understanding the formation of spatial lattice solitons [7–12]. Recently, many intriguing linear and nonlinear phenomena have been reported in deformed or anisotropic lattices [5,12]. In this letter, we demonstrate tunable self-shifting Bloch modes mediated by deformation of hexagonal lattices. We show that the Bloch modes can move laterally along any direction as determined by the orientation of the anisotropic lattice potential in the unit cell. Our results represent a convenient setting for studying fundamental wave dynamics in anisotropic periodic structures.

We start our analysis with the normalized Schrödinger equation describing electromagnetic wave propagation in linear media, where the periodic refractive index potential can be introduced. Under the slowly varying envelope approximation, the paraxial propagation along the z-axis for a monochromatic wave Ψ in the photonic lattice is governed by

$$\left(\frac{\partial}{\partial z} - \frac{i}{2}\nabla_{\perp}^2\right)\Psi = i\Delta n_l \Psi, \qquad (1)$$

where Ψ denotes the complex amplitude of the probe wave, $\nabla_{\perp}^2 = \partial_{xx} + \partial_{yy}$, and Δn_l is the periodic potential of the photonic lattice. Here we assume the index potential forms a hexagonal lattice (with lattice period d) with primitive axes $\mathbf{a}_1 = d\mathbf{i}$ and $\mathbf{a}_2 = 0.5d(\mathbf{i} + \sqrt{3}\mathbf{j})$, as

depicted in the left panel of Fig. 1(a). The transmission modes can be solved in the form $\Psi = b(x, y)\exp(i\beta z)$, where β is the propagation constant and $b(x, y)$ is the Bloch wave. For the Bloch wave vector $\mathbf{k} = k_x\mathbf{i} + k_y\mathbf{j}$, the corresponding Bloch wave $b(x, y)$ and propagation constant $\beta(\mathbf{k})$ (bandgap structure) can be obtained from Eq. (1). The first transmission band of a perfect hexagonal lattice is shown in the middle panel of Fig. 1(a), where six threefold-symmetric points at the bottom of the band are mapped out. Among these six points, there exist two
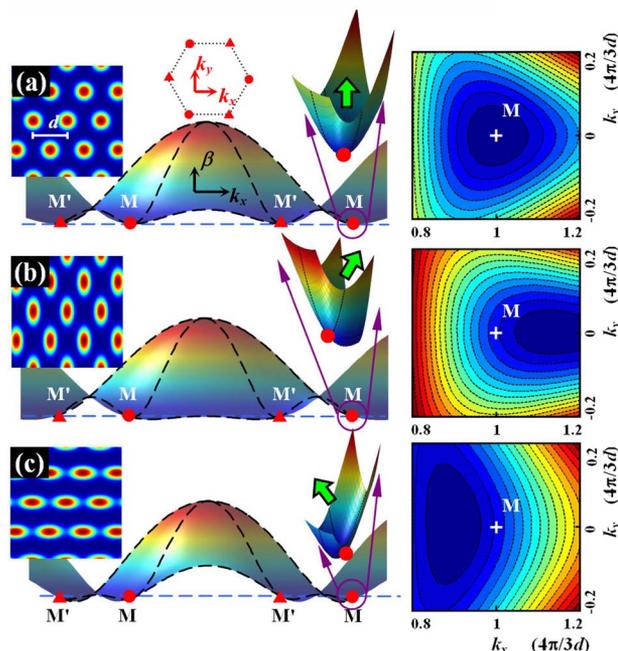

Fig. 1. (Color online) Diffraction curves of the first band in (a) perfect and (b), (c) anisotropic hexagonal lattices. Left, lattice structures; middle, diffraction curves; right, local distributions of the first band around the M-point. Insets show the local diffraction curves around the M-point.

degenerate modes associated with inversion-symmetry points M and M' (Fig. 1(a), circles and triangles, respectively). Here we focus on one of them to simplify the discussion.

The light refraction in the photonic lattice can be determined from $\gamma = \partial\beta/\partial\mathbf{k}$, which is the local slope of the diffraction curve. In a perfect hexagonal lattice, the point M is located at the bottom (minimum point) of the first band (see Fig. 1(a)), and the refraction of the corresponding Bloch mode $\gamma = 0$, i.e., the light propagates along the lattice waveguide without lateral shifting. This is a common property that most Bloch waves of high-symmetry points share. However, in anisotropic hexagonal lattices (e.g., elliptical index distribution in the unit cell), the diffraction curves are deformed (as shown in Figs. 1(b) and 1(c)) and the M-point is no longer the minimum, resulting in a nonzero γ. This indicates that the corresponding Bloch modes should move laterally during propagation. For an elliptical lattice potential (ellipticity ratio of 0.5) with major axis oriented in the vertical direction [Fig. 1(b)], the minimum point shifts aside to the right of the M-point, causing the Bloch waves to move toward the positive x-axis ($\gamma_x = \partial\beta/\partial k_x < 0$, $\gamma_y = \partial\beta/\partial k_y = 0$). Likewise, for an elliptical potential with major axis oriented in the horizontal direction (Fig. 1(c)), the minimum shifts to the left of the M-point and the Bloch waves move toward the negative x-axis ($\gamma_x > 0$, $\gamma_y = 0$).

It is worth mentioning that the deviations of the minimum points of transmission bands as represented above never happen in a lattice belonging to an orthorhombic system (e.g., a square lattice). In an orthorhombic system, because of the inversion and translational symmetry in k-space, the local diffraction curves around the high-symmetry points of the Brillouin zone always remain inversion-symmetric, even in an anisotropic lattice. This makes the high-symmetry points always stay at the maximum or minimum points (i.e., the zero-refraction positions) of the diffraction curves, and the corresponding Bloch waves cannot move transversely. Thus, the moving of the Bloch waves is a phenomenon particular to hexagonal lattices and can be considered a type of symmetry-breaking propagation in addition to that in [6].

The Bloch waves corresponding to the $\overline{M}$-point in Figs. 1(a)–1(c) are calculated as shown in the top of Figs. 2(a)–2(c), respectively, where the left and right panels are amplitude and phase distributions, respectively. To make clear how the energies flow, it is necessary to analyze the transverse Poynting vector $\mathbf{S}_\perp [\propto i(b\nabla_\perp b^* - b^*\nabla_\perp b)]$ associated with the Bloch waves, as depicted by the arrows in the bottom of Fig. 2. For a Bloch wave at the M-point of a perfect hexagonal lattice [Fig. 2(a)], every three adjacent wave humps form a vortex of unit topological charge, among which light energy flows evenly and maintains total balance. However, in the anisotropic hexagonal lattices, the balance of energy flow of the Bloch wave is broken [10] and the light energy of the Bloch wave flows laterally on the whole. It can be seen that the Bloch waves in Figs. 2(b) and 2(c) tend to move in opposite directions (rightward and leftward, respectively), as expected above. These Bloch waves are self-shifting modes without need of any additional "forces."
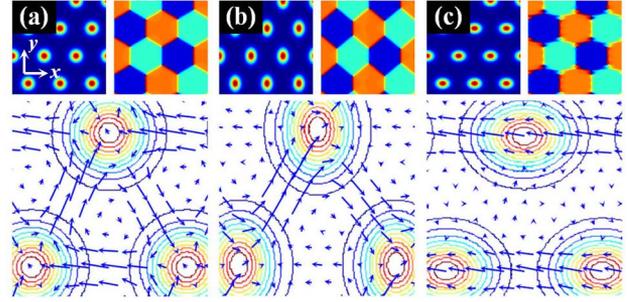

Fig. 2. (Color online) Bloch waves at the M-point corresponding to the lattice structures in Figs. 1(a)–1(c). Top, amplitude and phase distributions; bottom, transverse Poynting vectors of the Bloch waves.

The self-shifting modes are closely related to the orientations of the anisotropic lattice potential, which is defined as the angle θ between the long axis of the elliptical potential and the x-axis, as depicted in Fig. 3(a). To quantitatively analyze the self-shifting property, a normalized variable $\mathbf{F}(\theta)$ is introduced to characterize the total energy flow within the area of a single primitive cell, defined as $\mathbf{F}(\theta) = \iint_{\mathrm{cell}}\mathbf{S}_\perp(\theta)\mathrm{d}x\mathrm{d}y / \left|\iint_{\mathrm{cell}}\mathbf{S}_\perp(\theta)\mathrm{d}x\mathrm{d}y\right|_{\mathrm{max}}$. The amplitude and phase angle of $\mathbf{F}(\theta)$, which respectively represent the quantity and direction of the self-shifting, are calculated with the continuous variation of θ from 0° to 180° as shown in Fig. 3(b), where the solid and dashed lines correspond to $|\mathbf{F}|$ and arg $(\mathbf{F})$, respectively. The result shows that the shift direction of the M-point Bloch wave varies nearly linearly with the orientation of the lattice potential, with a periodic disturbance. Meanwhile, the displacement $|\mathbf{F}|$ varies periodically because of the sixfold symmetry of the hexagonal lattice, with the maximum and minimum (their ratio is about $1:0.55$) at $\theta = 0°$ (60°, 120°) and 30° (90°, 150°), respectively. In addition, the lattice potential and its ellipticity ratio can affect the shift magnitude rather than the shift direction, and a higher potential or a more intense anisotropy leads to stronger mobility of the Bloch modes. As a result, the self-shifting of the Bloch modes can be controlled by the anisotropy of the lattice structure.

It should be especially noted that these shiftings of the infinitely extended, z-independent Bloch waves cannot
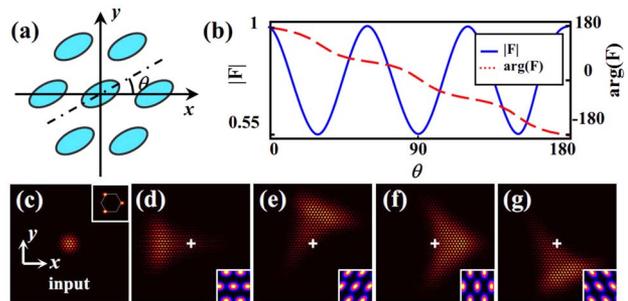

Fig. 3. (Color online) (a) Geometry of a typical anisotropic hexagonal lattice. (b) Displacement and direction of the shifting of the Bloch wave versus θ. (c) Input beam modulated with the M-point Bloch wave with its spectrum inserted. (d)–(g) Propagation in lattices with $\theta = 0°$, 45°, 90°, and 135°, respectively, with the input sites indicated by plus signs.
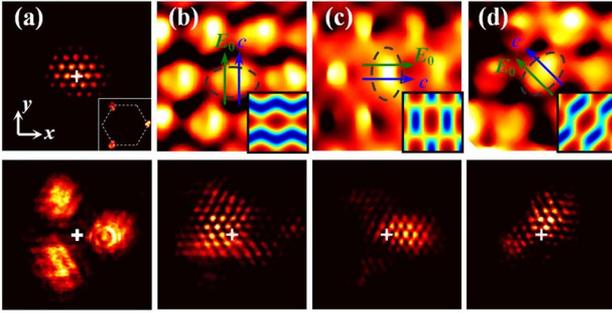
Fig. 4. (Color online) Experimental observation of the self-shifting Bloch modes in light-induced hexagonal lattices. (a) Geometry of the bias condition. (b) Input profile (top) and linear output without lattice (bottom); the inset shows the k-space spectrum. (c)–(e) Output beam profiles (bottom) in the anisotropic hexagonal lattices (top) under different bias conditions; insets depict the corresponding calculated lattice index profiles.

be observed directly. In order to visualize the self-shifting of the Bloch modes, the interference field of three planar waves with a circular Gaussian envelope is utilized as a probe beam to match the multivortex mode at the M-point, as shown in Fig. 3(c). The excited output profiles in the anisotropic lattices with $\theta = 0°$, $45°$, $90°$, and $135°$ are depicted in Figs. 3(d)–3(g), respectively. These results represent clearly the self-shifting properties of M-point Bloch modes, and the shift direction is determined by the orientation of the anisotropic lattice potential as expected according to Fig. 3(b). Furthermore, the output profiles deviate from the triangular shape as a result of the anisotropic local diffraction at the M-point (see Figs. 1(b) and 1(c), right).

To demonstrate the self-shifting modes experimentally, anisotropic hexagonal lattices were optically induced [3,12] in a strontium barium niobate crystal of size of $5 \text{ mm} \times 5(c) \text{ mm} \times 10 \text{ mm}$. Because of the intrinsic anisotropic nonlinearity [13, 14], the light-induced photonic lattices possess high anisotropy, which can be tuned by the bias condition [3,11,12]. Under the illumination of the hexagonal lattice beam [see the background of Fig. 4(a)], we applied the externally biased voltage (E_0) parallel to the c-axis and rotated the photorefractive crystal to establish anisotropic hexagonal lattices with different orientations, as shown in Fig. 4(a). The index distributions of the lattices are measured with digital holography [15, 16], as shown in the top of Figs. 4(c)–4(e). To compare with the results in Figs. 3(d), 3(f), and 3(e), the angles between E_0 (or the c-axis) and the x-axis in Figs. 4(c)–4(e) are set to $90°$, $0°$, and $135°$, respectively. The corresponding lattice index profiles are calculated with the anisotropic model [3,10–12], as shown in the insets of Figs. 4(c)–4(e). The probe multivortex beam is constructed by the interference of three beams with a method similar to [10], as shown in the top of Fig. 4(b). The spectrum of the probe beam is adjusted to coincide with that of the lattice beam (see Fig. 4(b), inset) to guarantee its on-axis propagation. Without the lattice, the probe beam evolves into three separate spots, with their center marked by a plus sign in the bottom of Fig. 4(b). Hence, the excited Bloch wave has no

lateral momentum. In the presence of anisotropic hexagonal lattices, after the excitation of the M-point Bloch modes, the probe beam moves laterally (i.e., with nonzero transverse momentum). The directions of movement are as expected. Apparently, in our experiment the mobility of the Bloch modes can be easily controlled by changing the bias condition. In addition, the output beam profiles shrink slightly in comparison with those at input as a result of anomalous diffraction of the probe beam [3].

To summarize, we have demonstrated controllable self-shifting Bloch modes in anisotropic hexagonal lattices. Because of the anisotropic lattice potential, the minimum points of the first transmission band (band edge) deviate from the high-symmetry M-points, leading to the shifting of the M-point Bloch modes. The shift direction is determined by the orientation rather than the index modulation, as well as by the ellipticity of the anisotropic lattice potential. The tunable self-shifting modes have been experimentally observed in optically induced hexagonal lattices. These wave phenomena are expected to occur in other periodic systems with similar symmetry.

References

1. D. N. Christodoulides, F. Lederer, and Y. Silberberg, Nature **424**, 817 (2003).
2. A. A. Sukhorukov, D. Neshev, W. Krolikowski, and Y. S. Kivshar, Phys. Rev. Lett. **92**, 093901 (2004).
3. P. Zhang, C. Lou, S. Liu, J. Zhao, J. Xu, and Z. Chen, Opt. Lett. **35**, 892 (2010).
4. O. Peleg, G. Bartal, B. Freedman, O. Manela, M. Segev, and D. N. Christodoulides, Phys. Rev. Lett. **98**, 103901 (2007).
5. O. Bahat-Treidel, O. Peleg, and M. Segev, Opt. Lett. **33**, 2251 (2008).
6. S. Liu, Y. Hu, P. Zhang, X. Gan, C. Lou, D. Song, J. Zhao, J. Xu, and Z. Chen, Appl. Phys. Lett. **100**, 061907 (2012).
7. J. W. Fleischer, M. Segev, N. K. Efremidis, and D. N. Christodoulides, Nature **422**, 147 (2003).
8. C. Lou, X. Wang, J. Xu, and Z. Chen, Phys. Rev. Lett. **98**, 213903 (2007).
9. X. Wang, Z. Chen, J. Wang, and J. Yang, Phys. Rev. Lett. **99**, 243901 (2007).
10. B. Terhalle, T. Richter, A. S. Desyatnikov, D. N. Neshev, W. Krolikowski, F. Kaiser, C. Denz, and Y. S. Kivshar, Phys. Rev. Lett. **101**, 013903 (2008).
11. Y. Hu, C. Lou, P. Zhang, J. Xu, J. Yang, and Z. Chen, Opt. Lett. **34**, 3259 (2009).
12. P. Zhang, J. Zhao, F. Xiao, C. Lou, J. Xu, and Z. Chen, Opt. Express **16**, 3865 (2008).
13. P. Zhang, S. Liu, C. Lou, Y. Gao, J. Zhao, J. Xu, and Z. Chen, Appl. Phys. B **95**, 559 (2009).
14. P. Zhang, J. Zhao, C. Lou, X. Tan, Y. Gao, Q. Liu, D. Yang, J. Xu, and Z. Chen, Opt. Express **15**, 536 (2007).
15. J. Zhao, P. Zhang, J. Zhou, D. Yang, D. Yang, and E. Li Chin, Phys. Lett. **20**, 1748 (2003).
16. P. Zhang, D. Yang, J. Zhao, K. Su, J. Zhou, B. Li, and D. Yang, Chin. Phys. Lett. **21**, 1558 (2004).